RESEARCH ARTICLE

Therapeutic response to bronchial thermoplasty: toward feasibility of patient selection based on modeling predictions

G. M. Donovan,[1] P. B. Noble,[2] and D. Langton[3]

[1]*Department of Mathematics, The University of Auckland, Auckland, New Zealand;* [2]*School of Human Sciences, The University of Western Australia, Crawley, Western Australia, Australia;* and [3]*Faculty of Medicine, Nursing and Allied Health, Monash University, Melbourne, Victoria, Australia*

Abstract

Bronchial thermoplasty (BT) is a treatment for moderate-to-severe asthma in which the airway smooth muscle layer is targeted directly using thermal ablation. Although it has been shown to be safe and effective in long-term follow-up, questions remain about its mechanism of action, patient selection, and optimization of protocol based on structural phenotype. Using a cohort of 20 subjects who underwent thermoplasty and assessment by computed tomography (CT), we demonstrate that response to BT can be feasibly predicted based on pretreatment airway dimensions that inform a subject-specific computational model. Analysis revealed the need for CT assessment at total lung capacity, rather than functional residual capacity, which was less sensitive to the effects of BT. Final model predictions compared favorably with observed outcomes in terms of airway caliber and asthma control, suggesting that this approach could form the basis of improved clinical practice.

NEW & NOTEWORTHY Bronchial thermoplasty is a treatment for asthma that targets the airway smooth muscle directly. We demonstrate the feasibility and constraints of predicting patient-specific response to thermoplasty using a computational model informed by pretreatment CT scans at different lung volumes. Predictions are compared with functional outcomes and posttreatment CT scans. This has the potential to form the basis for improved clinical practice.

airway hyperresponsiveness; airway smooth muscle; asthma; computational modeling

INTRODUCTION

Bronchial thermoplasty (BT) is a treatment for moderate-to-severe asthma in which the airway smooth muscle (ASM) layer is targeted directly using thermal ablation, delivered by radiofrequency probe and bronchoscope (1–3). BT has been shown to be safe and effective, with consistent improvements in patient-reported outcomes (i.e., questionnaire scores) at follow-up periods as long as 10 years (4). Clinical willingness to prescribe BT is however limited relative to the vast number of potential patients with severe or hard-to-treat asthma. The explanation for underuse is twofold: *1*) coincident development of monoclonal antibody therapies as an alternative treatment, which is a clear clinical success story and *2*) our lack of physiological insight into mechanism of action and appropriate patient selection, which is an outstanding and pressing question in respiratory research.

Over the past few years there has been mounting and encouraging evidence supporting real physiological changes after BT (5–8), which provides opportunity for patient selection and even customizing protocols based on structural or functional phenotypes (9, 10). Notably, aggregate airway volume on CT is increased after BT (11) and we have demonstrated changes at the individual airway level throughout the bronchial tree that is accessible by CT (8). We therefore now have an approach that is sensitive to BT with the potential for further refinement. Previous CT measurements were performed at total lung capacity (TLC) which may partially normalize airway caliber in asthmatic patients. Several studies (12, 13) have shown that although the capacity to expand the airway is similar in subjects with and without asthma, the former does not benefit from the same bronchodilation on return to functional residual capacity (FRC). Thus, it may be that resolution of the asthma phenotype after BT could be better assessed by CT performed at FRC.

The present study builds on the above methodology and considers the feasibility of examining future patient response based on pretreatment airway dimensions. First, we replicated our previous analysis on CT-derived airway dimensions, this time using scans at FRC and performed a direct comparison with scans at TLC to establish which approach is most sensitive to the effects of BT. Based on the outcome of this analysis, pretreated airway dimensions were used in a patient-specific computational model to predict individual response to BT, and we compared these predictions with empirical changes after BT. Findings demonstrate the feasibility of patient-specific predictions to inform patient selection for BT. A patient-specific strategy

1341

offers the potential of improved outcomes, compared with generic or phenotype-level approaches.

METHODS

Human Ethics and Recruitment

Prospective approval to undertake the study was given by the Peninsula Health Human Research Ethics Committee and no patient was enrolled without having given informed consent. Participants (n = 20) were referred for BT from a tertiary hospital severe asthma clinic. To be considered for BT, patients needed to be using inhaled triple therapy and have poorly controlled symptoms with frequent oral steroid requiring exacerbations. All participants were also required to meet the European Respiratory Society/American Thoracic Society (ERS/ATS) definition of severe asthma, and have excluded alternative respiratory conditions such as COPD or bronchiectasis [14].

Clinical Measurements

For all patients, the following data were recorded: age, sex, weight, height, asthma medication usage, asthma exacerbation history, lung function parameters, and the 5-item asthma control questionnaire (ACQ) [15]. Key clinical outcome parameters included changes measured at 6 and 12 mo in 1) ACQ, 2) pre-bronchodilator forced expiratory volume in 1 s (FEV_1), 3) short acting beta-agonist (SABA) usage (measured in puffs/day), 4) daily maintenance oral corticosteroid (OCS) dose (measured in mg/day of prednisolone), and 5) the number of oral steroid requiring exacerbations of asthma reported in the previous 6 mo. Patient assessments were performed by experienced clinical research nursing and scientific staff, and were conducted independently of the procedural team. Spirometry was performed using the Jaegar Masterscreen Body (Carefusion, Hoechberg, Germany) and tests were conducted in the morning, and having withheld bronchodilators since the previous evening. The laboratory equipment was calibrated on the morning of testing and all tests were conducted to ERS/ATS standards [16]. The predicted value equations used were taken from the Global Lung Initiative [17].

Baseline Characteristics

Participants comprised 7 males, 13 females who were 56.0 ± 14.3 yr with a body mass index (BMI) 32.9 ± 7.6 kg/m^2. The mean ACQ score was 3.5 ± 0.9. Seventeen of the 20 patients were being treated with maintenance oral prednisolone—group mean dose 15.3 ± 15.3 mg/day. All patients were using triple inhaler therapy with beclomethasone-equivalent inhaled steroid dose $1,750 \pm 786$ μg/day. The frequency of exacerbations requiring OCS in the 6 mo before BT was 2.8 ± 2.1.

The mean pre-bronchodilator FEV1 was 44.5 ± 14.0% predicted, with an average improvement of 15.4 ± 16.1% after 400 μg salbutamol. Vital capacity was 70.9 ± 14.9% predicted, and the forced expiratory ratio was 52.2 ± 12.2%.

Experimental Protocol

CT was conducted at baseline, at a mid-treatment timepoint (see below) and 12 mo after completion of all BT procedures. BT was performed under general anesthesia with patients routinely observed in hospital overnight postprocedure. For the purposes of this study, the scheduling of the BT procedures was altered in a novel way to achieve one treated lung (left side) and one untreated lung (right side) at the mid-treatment timepoint. The left lower lobe was treated in the first BT session, and then the left upper lobe in the second session. CT assessment at the mid-treatment timepoint was conducted four weeks after completion of BT treatment to the left lung, and therefore before treatment of the right lung (which acted as a control). Following the second set of imaging, the right lower and upper lobes were treated together in the final BT session, which preceded 12-mo CT assessment. Consistent with current guidelines, the right middle lobe was not treated.

CT Imaging and Analysis

Noncontrast CT scanning was performed on a 128-slice Siemens Definition AS+ scanner with a helical slice thickness of 0.6 mm, rotation time of 0.6 s, detector coverage of 38.4 mm, and tube voltage of 100 kV. Scans were performed at FRC and TLC in a stable state, pre-bronchodilator, and before peri-procedural oral steroid administration.

The image analysis process was semi-automatic and performed blind to both patient and treatment condition by the same operator. The airway tree was segmented from the CT source data using the tube segmentation framework [18] as implemented in CustusX v18.04 [19] (SINTEF Digital, Trondheim, Norway). Centerlines for the segmented airways were obtained concurrently. The process was almost fully automatic except for the determination of a segmentation "seed point" placed manually in the trachea for scans in which fully automatic segmentation failed. Segmentation of the airways other than the trachea was not sensitive to seed point placement, and the tracheal segmentation is not used in the analysis. After segmentation and centerlining the analysis process was fully automatic. Segmented volume is sensitive to changes in detected airway length, but this is mitigated by the robustness of the segmentation algorithm [18] and the stability of the segmented airway length [8]. In addition, our analyses are based on cross-sectional area rather than volume itself, which is less sensitive to detected length.

Pairs of airway tree segmentations were registered by rigid transformation using the coherent point drift algorithm [20] as implemented in Matlab R2020b (Mathworks, Natick, MA). Airway centerlines were transformed according to the same rigid transformation, and then airways were matched according to the transformed centerlines. The deviation between two transformed centerlines was defined to be the 2 norm of the segment difference normalized by the average segment length. Airway lumen volumes were determined by assigning points in the segmentation point cloud to the nearest airway centerline. An example of matched segmentations is shown in Fig. 1, with pretreatment on the left and posttreatment on the right; colors indicate matched airways, whereas black airways are unmatched.

The analysis process was repeated for all scan pairs. Eighteen patients completed their treatment and hence each had three scan pairs available for analysis: pre → mid, mid → post, and pre → post; totaling 54 scan pairs.
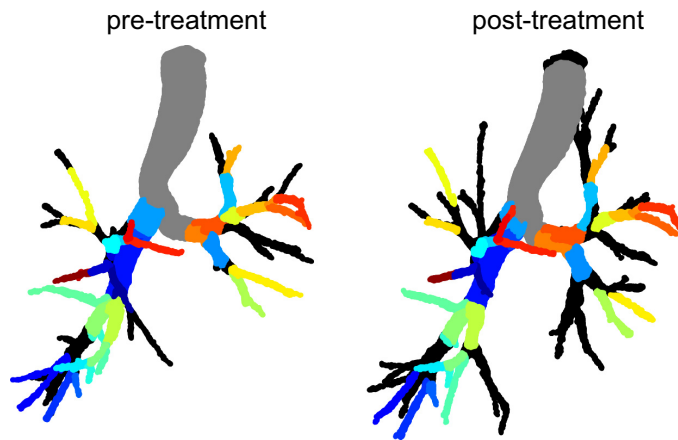
pre-treatment   post-treatment

Figure 1. Illustration of airway tree segmentation and matching for a single subject (No. 5) at TLC. *Left*: segmentation from pretreatment scan; *right*: segmentation from posttreatment scan. Colors indicate matched airways, whereas black airways are unmatched. TLC, total lung capacity.

Including two additional patients who only reached mid-treatment, a further two scan pairs were available i.e., 56 pairs in total. Note that because the scans are analyzed in pairs, the matched airways from one scan pair (e.g., pre → mid) will not necessarily be the same as the airways matched in the other pairs (pre → post and mid → post).

Subject-Specific Modeling

We adapted a previously developed mathematical model of BT (21), but now in a subject-specific context. The computational geometry was determined from the CT segmentation out to the segmentation limits, and the lobar surfaces were also segmented as described in the METHODS. Conducting airways between the airway segmentation limit and the periphery were reconstructed algorithmically as described previously (21, 22). Airway structural properties were generated using a statistical model fitted to extensive structural airway data. The measurements of these airways, in terms of epithelial basement membrane perimeter, airway wall area, ASM area and anatomical level, are used to inform a statistical model of airway structure at each airway order, as analyzed previously (21).

Within this airway tree structure, we calculate volume, flow and impedance within intraparenchymal airways. Multiple independent simulations are then performed, at varying doses of contractile agonist, and the response in airway volume and resistance determined. The simulations are then repeated with a 75% reduction in ASM mass, which has been demonstrated to approximate the effects of BT (23). A total of 2,880 simulations were performed across 5 subjects (a subset due to high computational cost) using $60\times$ Intel Xeon Gold 6126 cores. The 5 subjects were selected on the basis of their automatic airway segmentation centerlines being suitable for direct modeling—the remaining subjects require manual correction. For each subject, the 2.5% of simulations with the smallest root-mean-square error of the matched airways between pretreatment CT observations and pretreatment model simulations were included in the final analysis. An example of a pre- and posttreatment simulation pair is shown in

Fig. 2, showing normalized flow in each airway segment compared between pretreatment (*left*) and posttreatment (*right*). Although this is only a single example, the observed decrease in ventilation heterogeneity is typical (21). Sensitivity analyses to the assumed BT ablation percentage (23) and other model parameters (24) have been reported previously.

Statistical Analysis

Matlab R2020b was used for statistical analyses. Normally distributed data are reported as means ± standard deviation and a t test was used; nonparametric data are reported as median (interquartile range) and the sign test was used. Changes in airway area were analyzed using two-way repeated-measures ANOVA with lung volume and timepoint as factors (unbalanced design, type II sum of squares). Correlation between change in ACQ and change in model predicted resistance were assessed with Kendall's τ. In all cases statistical significance was taken at $P < 0.05$.

RESULTS

Clinical Response to BT

The clinical response to BT of the 18 patients who completed 12 mo follow up is described in detail in ref. (8). Significant improvements were observed in ACQ ($P = 0.001$), exacerbation frequency ($P = 0.020$) and use of oral steroids ($P = 0.030$), and SABA ($P = 0.001$). A trend towards improvement in FEV_1 (% predicted) did not reach statistical significance ($P = 0.065$).

Analysis of Scans at FRC

Change in matched individual airway area on CT scans performed at FRC and TLC are shown in Fig. 3. Results in Fig. 3 are color-coded as left lung (red), right lung (green), both (gray), with FRC in the lighter tone and TLC in the darker tone. Figure 3A shows comparison of scans between pretreatment and mid-treatment timepoints, in which only the left lung has been treated. Figure 3B shows the scans comparing mid treatment with post treatment timepoints, the period in which the right lung is treated (excluding the right middle lobe). Figure 3C shows the comparison between pretreatment and posttreatment scans, in which both lungs are treated. Finally, Fig. 3D shows the combined results for both sides in the pre-post scan comparisons; here the changes at TLC are significant ($P = 0.019$ by one sample t test) but not at FRC. The results at TLC have been previously reported (8) but are shown here for direct comparison and inclusion in a two-way analysis. It is important to note that, because the scans are matched as pairs, and only a subset of airways can be matched in each scan pair, there is not a simple additive relationship between the pre-mid, mid-post and pre-post scans, because different airways may be matched for each scan pair; the total number of matched airways in each case is indicated in Fig. 3.

A two-way repeated-measures ANOVA was performed for each lung with volume (FRC/TLC) and timepoint (pre → mid, mid → post, pre → post) factors. In the right lung there was a significant main effect for timepoint ($F = 3.4$, $P = 0.046$), no significant main effect for volume ($P = 0.55$), and

Figure 2. Example pre- and posttreatment simulation pair (Subject No. 5) in the simulated left lung illustrating the characteristic reduction in ventilation heterogeneity after BT (21). Color scale shows ventilation normalized to nominal (21). BT, bronchial thermoplasty.
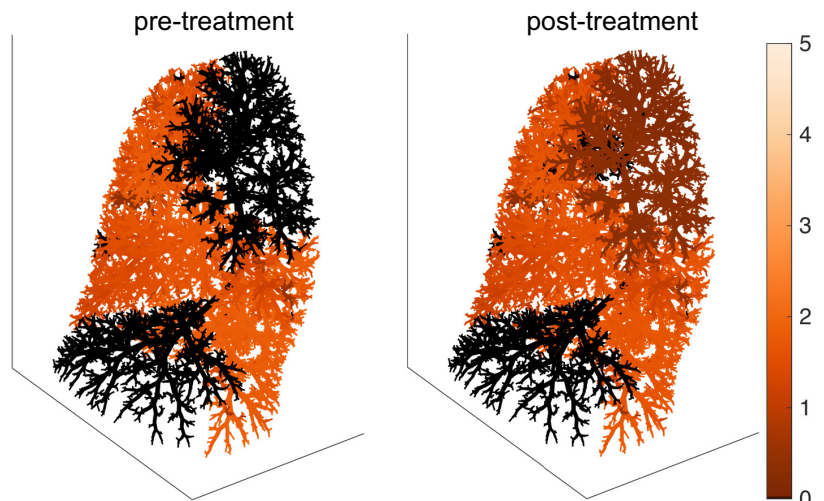
no interaction (P = 0.18). Post hoc assessment indicated significant increases in matched airway area only between TLC pre-mid and TLC mid-post, and TLC pre-mid and TLC pre-post groups, in concordance with the treatment of the right lung between the mid and post scans.

In the left lung, the two-way repeated-measures ANOVA indicated no significant main effect for timepoint, volume or interaction. One possible explanation for the lack of timepoint effect on the left side is the timing of the mid-treatment scan at 4 wk after the treatment of the left upper lobe, at which time the acute effects of treatment may not have fully resolved (5); if so, then the full treatment effect is apparent only in the pre → post timepoint and there is no fully untreated control timepoint for comparison on the left side.

Broadly, the above supports the prior conclusion that BT induces airway dilation of ∼5%–7% in terms of airway area, but that CT scans at TLC are more sensitive to these changes than CT scans at FRC. This sensitivity is likely affected by the number of airways which can be matched; at TLC the average is ∼25 matched airways per scan pair, whereas at FRC, this falls to 18. On the overall basis of increased diagnostic sensitivity, the TLC scans are used as the input for the subject-specific models that follow.

Subject-Specific Modeling

The results of the subject-specific lung models are shown in Fig. 4 for 5 subjects, aggregated from 2,880 total simulations. The left-hand column shows the posttreatment airway size for the airways directly measurable with CT; posttreatment model prediction envelopes, based on the pretreatment TLC scans, are shown in the gray boxplots, whereas corresponding posttreatment CT measurements for the matched airway are indicated by the red circles. Note that for reasons of computational cost and availability of histology data for calibration, only the left lung is simulated (21). Here "airway index" is an arbitrary labeling of the matched airways.

The right-hand column gives the simulated dose-response curves for each subject, comparing pretreatment (blue) and posttreatment (red) simulations. Error bars give the standard deviation. As previously reported in the generic case (i.e.,

not subject-specific) (21), predicted improvements in resistance are negligible at baseline but increase with agonist stimulation.

All five subjects show strongly significant predictions of BT-induced improvement in resistance at modest and high levels of agonist stimulation, and all five subjects were indeed categorized as BT responders with changes in ACQ ranging from 1.2 to 3.8 (where 0.5 is the minimum clinically significant difference). Further, the model predicted changes in resistance in the left lung at high levels of agonist stimulation correlate significantly (P = 0.03, Kendall's correlation coefficient 0.95) with observed subject change in ACQ from pretreatment to mid-treatment. Recall that only the left lung is modeled and that the left lung is treated first and is thus the most relevant comparison. Model predicted resistance changes do not correlate significantly with the pretreatment to posttreatment (both lungs treated) change in ACQ at either high or low agonist stimulation (P > 0.3), nor pre-mid at lower levels of agonist stimulation (P = 0.13). However, given the small sample size these should be treated with appropriate caution.

DISCUSSION

We have demonstrated that subject-specific modeling of BT from pretreatment CT is feasible. The vast majority of posttreatment CT airway size observations lie within the prediction envelopes based only on pretreatment and population-level data (see Fig. 4). However, the prediction range is relatively large, due to the relatively limited data which can be obtained from the pretreatment CT (24). ASM area, for example, cannot be measured directly from CT, even for the largest airways, and thus some input parameters must be inferred from population-level statistical models (21). This uncertainty contributes substantially to the computational time and effort, which at present is a barrier preventing translation to the clinic. In the current approach, the large input uncertainty requires very significant oversampling (by a factor of 40) to calibrate the pretreatment model; by narrowing this uncertainty with additional pretreatment measurements, both the output uncertainty and the computational cost will be reduced.
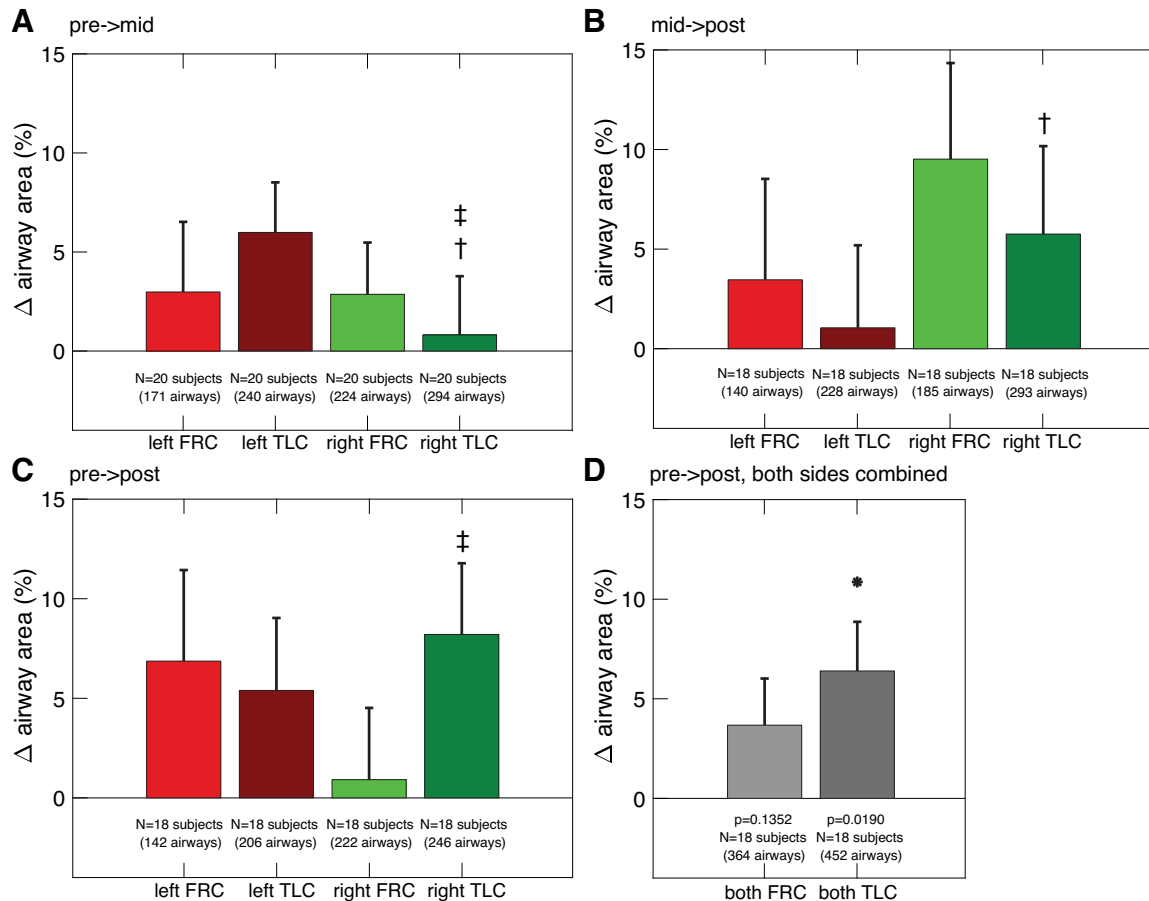
Figure 3. Results of matched airway analysis—% change in airway cross-sectional lumen area, means ± SE; †‡Groups differ pairwise by post hoc test following two-way repeated-measures ANOVA on each side, *$P < 0.05$ by one sample t test. Between pretreatment and mid-treatment assessments (*A*), the left lung is treated and the right remains untreated; between mid-treatment and posttreatment (*B*), the right lung is treated. The pre → post pair assessment (*C* and *D*) captures treatment of both sides. Results are color-coded as left lung (red), right lung (green), both (gray), with FRC in the lighter tone and TLC in the darker tone. Data are subject-aggregated, but the total number of matched airways in each case is shown to emphasize that because scans are analyzed in pairs, the matched airways from one scan pair will not necessarily be the same as the airways matched in the other pairs, and further that the number of matched airways is greater at TLC than at FRC. FRC, functional residual capacity; TLC, total lung capacity.

At present, the latter requires several months of computation for each subject-specific prediction,[1] which is not clinically practicable.

Although these computational constraints could be mitigated either by technical improvements to the algorithms or application of greater computing resources, a better approach would be to acquire additional pretreatment data. Pretreatment information such as ASM area acquired by polarization-sensitive optical coherence tomography (PS-OCT) (25–27) would offer significant improvement in the predictive accuracy by narrowing the possible range of pretreatment states, at least in the larger airways (24). The improved prognostic power afforded by ASM area in turn reduces the computational cost, which would facilitate a larger study to demonstrate more robustly the relationship between model and patient outcomes. For example, the change in resistance at high agonist doses correlates with improved (lowered) ACQ, but given the small sample size this should be treated with appropriate caution before confirmation in a larger cohort.

Direct analysis of individual airway response from CT scans at FRC show the same trends as previously demonstrated at TLC, in which airways dilated by ∼6%–7% overall and as much as 13% in the smallest airway quintile (8), but here assessed at FRC fail to reach statistical significance. As acknowledged in the methods and results, changes across time (pre → mid, mid → post, and pre → post) will not be cumulative, and should be interpreted with this methodological limitation in mind. The rationale for assessing changes after BT using CT scans at FRC was initially motivated by prior observations that this operating volume more clearly distinguishes airway abnormalities in patients with asthma compared with control (12, 13). Also, FRC could theoretically be more sensitive to these changes because of nonlinear compliance differences (i.e., greater compliance at transmural pressures near FRC compared with those near full inflation) (28, 29), but any such advantage appears to be outweighed by differences in the number of airways segmented. Given that the imaging resolution is fixed, and all relevant structures are

Fn1

---

[1]Using substantial computing power (60× Intel Xeon Gold 6126 cores) but relatively unoptimized research MATLAB code.
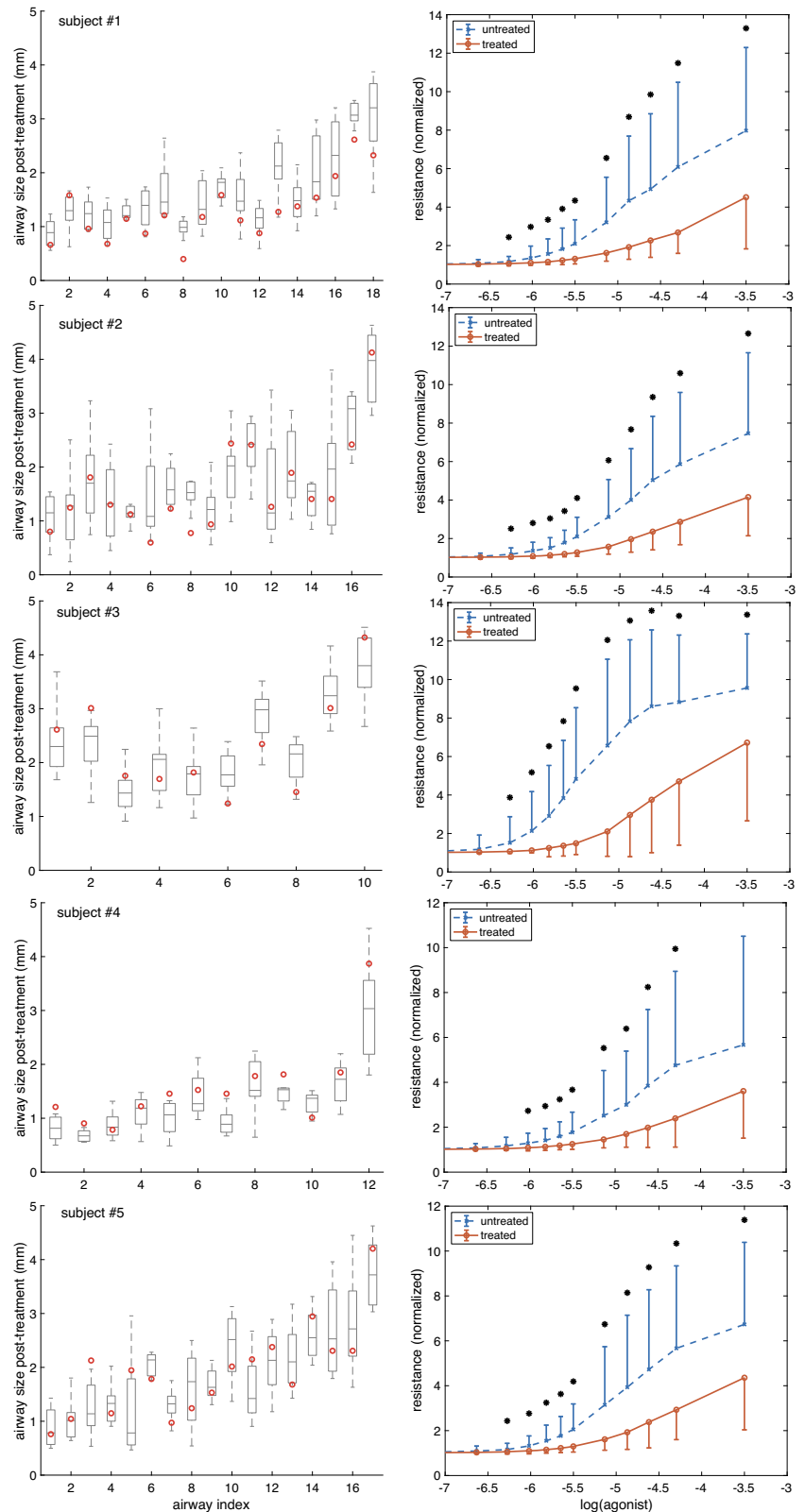
Figure 4. Subject-specific simulation results for 5 subjects. Each row is a subject. *Left*: posttreatment airway sizes, model predictions (based on pretreatment scans) in gray boxplots, actual CT measurements as red circles. *Right*: model predictions of pre- and posttreatment resistance dose-response curves. *$P < 0.01$ by nonparametric Mann–Whitney U test.

smaller at FRC than at TLC, fewer airways can be segmented and thus matched, and as a result the overall statistical power is reduced. Overall, ~28% fewer airways can be matched at FRC compared with TLC. Comparison on the basis of the same number of segmented airways is complicated by the fact that the loss of segmented airways at FRC is predominately in the smaller airways and so like-for-like comparison would require cross-volume matching

(see below). Thus, for the purpose of airway matching based on volume, TLC appears to be preferred over FRC.

FRC scans could, in principle, be used in conjunction with TLC scans to assess compliance changes in matched airways. In this case, it is not a simple case of matching a single scan pair, but four scans: FRC pretreatment, TLC pretreatment, FRC posttreatment, and TLC posttreatment. Not only does this increase the difficulty by requiring additional matches, the methodology for FRC-TLC matching is significantly more challenging. Volume-matched scans (FRC-FRC or TLC-TLC) can be compared by rigid transformation, essentially only correcting translation and rotation for position of the subject within the scanner. FRC-TLC matching, on the other hand, requires a more challenging deformable registration (30–32). Obtaining sufficient registration and matching quality to facilitate this mixed-volume analysis remains an area for future work. FRC scans could also be used in conjunction with TLC scans for other analyses such as measures of lung deformation, or to make a more direct comparison of volume-sensitivity in BT response by controlling for the number and size of the segmented airways (as above).

The implication of this research is that once a properly informed prognostic model is developed, patients can be screened as to their suitability for BT. CT scans at TLC are already performed before procedure to exclude a diagnosis of bronchiectasis (33), providing an opportunity to simultaneously quantify airway dimensions and therefore to assess the potential therapeutic benefit of BT. In the event that predictive modeling does not identify a likely benefit of BT, patients could be prevented from undergoing an invasive procedure that carries high short-term costs. Additional CT scans at FRC are an additional radiation burden beyond standard practice, which are not currently justified based on this analysis but may be useful in other ways (see above).

In conclusion, although scans at FRC theoretically offer additional information, for these purposes those at TLC both demonstrate treatment effects directly and can be used to inform subject-specific models. These subject-specific models may be used to offer personalized therapies in future, either in terms of patient selection or airway selection. However, the structural information offered by CT is at the boundary of feasibility in this regard; additional pretreatment data, potentially from PS-OCT, would enable a substantial reduction in both prediction uncertainty and computational cost, both of which would contribute to viability in a clinical setting. The methodology employed here could also potentially be applied in future to other therapies which alter airway structure, for example by pharmacological means (34).

GRANTS

DISCLOSURES

No conflicts of interest, financial or otherwise, are declared by the authors.

AUTHOR CONTRIBUTIONS

REFERENCES

1. **Castro M, Rubin AS, Laviolette M, Fiterman J, De Andrade Lima M, Shah PL, Fiss E, Olivenstein R, Thomson NC, Niven RM, Pavord ID, Simoff M, Duhamel DR, McEvoy C, Barbers R, Ten Hacken NHT, Wechsler ME, Holmes M, Phillips MJ, Erzurum S, Lunn W, Israel E, Jarjour N, Kraft M, Shargill NS, Quiring J, Berry SM, Cox G; AIR2 Trial Study Group.** Effectiveness and safety of bronchial thermoplasty in the treatment of severe asthma: a multicenter, randomized, double-blind, sham-controlled clinical trial. *Am J Respir Crit Care Med* 181: 116–124, 2010. doi:10.1164/rccm.200903-0354OC.

2. **Cox G, Miller JD, McWilliams A, FitzGerald JM, Lam S.** Bronchial thermoplasty for asthma. *Am J Respir Crit Care Med* 173: 965–969, 2006. doi:10.1164/rccm.200507-1162OC.

3. **Pavord ID, Cox G, Thomson NC, Rubin AS, Corris PA, Niven RM, Chung KF, Laviolette M; RISA Trial Study Group.** Safety and efficacy of bronchial thermoplasty in symptomatic, severe asthma. *Am J Respir Crit Care Med* 176: 1185–1191, 2007. doi:10.1164/rccm.200704-571OC.

4. **Chaudhuri R, Rubin A, Sumino K, Lapa E Silva JR, Niven R, Siddiqui S, Klooster K, McEvoy C, Shah PL, Simoff M, Khatri S, Barbers R, Mark Grubb G, McMullen EA, Olson JL, Laviolette M, BT10+ Study Group.** Safety and effectiveness of bronchial thermoplasty after 10 years in patients with persistent asthma (BT10+): a follow-up of three randomised controlled trials. *Lancet Respir Med* 9: 457–466, 2021. doi:10.1016/S2213-2600(20)30408-2.

5. **Goorsenberg AWM, d'Hooghe JNS, de Bruin DM, van den Berk IAH, Annema JT, Bonta PI.** Bronchial thermoplasty-induced acute airway effects assessed with optical coherence tomography in severe asthma. *Respiration* 96: 564–570, 2018. doi:10.1159/000491676.

6. **Langton D, Bennetts K, Noble P, Plummer V, Thien F.** Bronchial thermoplasty reduces airway resistance. *Respir Res* 21: 76, 2020. doi:10.1186/s12931-020-1330-5.

7. **Langton D, Bennetts K, Thien F, Plummer V, Noble PB.** Bronchial thermoplasty reduces ventilation heterogeneity measured by multiple breath nitrogen washout. *Respir Res* 21: 308, 2020. doi:10.1186/s12931-020-01575-x.

8. **Langton D, Noble PB, Donovan GM.** Response of individual airways in vivo to bronchial thermoplasty. *J Appl Physiol (1985)* 130: 1205–1213, 2021. doi:10.1152/japplphysiol.00959.2020.

9. **Donovan GM, Elliot JG, Boser SR, Green FH, James AL, Noble PB.** Patient-specific targeted bronchial thermoplasty: predictions of improved outcomes with structure-guided treatment. *J Appl Physiol (1985)* 126: 599–606, 2019. doi:10.1152/japplphysiol.00951.2018.

10. **Hall CS, Quirk JD, Goss CW, Lew D, Kozlowski J, Thomen RP, Woods JC, Tustison NJ, Mugler JP, Gallagher L, Koch T, Schechtman KB, Ruset IC, Hersman FW, Castro M.** Single-session bronchial thermoplasty guided by 129Xe magnetic resonance imaging: a pilot randomized clinical trial. *Am J Respir Crit Care Med* 202: 524–534, 2020. doi:10.1164/rccm.201905-1021OC.

11. **Langton D, Banks C, Noble P, Plummer V, Thien F, Donovan G.** The effect of bronchial thermoplasty on airway volume measured 12 months post procedure. *ERJ Open Res* 6: 00300-2020, 2020. doi:10.1183/23120541.00300-2020.

12. **Brown RH, Scichilone N, Mudge B, Diemer FB, Permutt S, Togias A.** High-resolution computed tomographic evaluation of airway distensibility and the effects of lung inflation on airway caliber in healthy subjects and individuals with asthma. *Am J Respir Crit Care Med* 163: 994–1001, 2001. doi:10.1164/ajrccm.163.4.2007119.

13. **Hulme KM, Salome CM, Brown NJ, Berend N, Agus HM, Horlyck KR, King GG, Chapman DG.** Deep inspiration volume and the impaired reversal of bronchoconstriction in asthma. *Respir Physiol Neurobiol* 189: 506–512, 2013. doi:10.1016/j.resp.2013.08.015.

14. **Chung KF**, **Wenzel SE**, **Brozek JL**, **Bush A**, **Castro M**, **Sterk PJ**, **Adcock IM**, **Bateman ED**, **Bel EH**, **Bleecker ER**, **Boulet L-P**, **Brightling C**, **Chanez P**, **Dahlen S-E**, **Djukanovic R**, **Frey U**, **Gaga M**, **Gibson P**, **Hamid Q**, **Jajour NN**, **Mauad T**, **Sorkness RL**, **Teague WG.** International ERS/ATS guidelines on definition, evaluation and treatment of severe asthma. *Eur Respir J* 43: 343–373, 2014 [Erratum in *Eur Respir J* 43: 1216, 2014]. doi:10.1183/09031936.00202013.

15. **Juniper EF**, **Svensson K**, **Mörk A-C**, **Ståhl E.** Measurement properties and interpretation of three shortened versions of the asthma control questionnaire. *Respir Med* 99: 553–558, 2005. doi:10.1016/j.rmed.2004.10.008.

16. **Miller MR**, **Hankinson J**, **Brusasco V**, **Burgos F**, **Casaburi R**, **Coates A**, **Crapo R**, **Enright P**, **van der Grinten CPM**, **Gustafsson P**, **Jensen R**, **Johnson DC**, **MacIntyre N**, **McKay R**, **Navajas D**, **Pedersen OF**, **Pellegrino R**, **Viegi G**, **Wanger J**; **ATS/ERS Task Force.** Standardisation of spirometry. *Eur Respir J* 26: 319–338, 2005. doi:10.1183/09031936.05.00034805.

17. **Cooper BG**, **Stocks J**, **Hall GL**, **Culver B**, **Steenbruggen I**, **Carter KW**, **Thompson BR**, **Graham BL**, **Miller MR**, **Ruppel G**, **Henderson J**, **Vaz Fragoso CA**, **Stanojevic S.** The Global Lung Function Initiative (GLI) Network: bringing the world's respiratory reference values together. *Breathe (Sheff)* 13: e56–e64, 2017. doi:10.1183/20734735.012717.

18. **Reynisson PJ**, **Scali M**, **Smistad E**, **Hofstad EF**, **Leira HO**, **Lindseth F**, **Nagelhus Hernes TA**, **Amundsen T**, **Sorger H**, **Langø T.** Airway segmentation and centerline extraction from thoracic CT–comparison of a new method to state of the art commercialized methods. *PLoS One* 10: e0144282, 2015. doi:10.1371/journal.pone.0144282.

19. **Askeland C**, **Solberg OV**, **Bakeng JBL**, **Reinertsen I**, **Tangen GA**, **Hofstad EF**, **Iversen DH**, **Våpenstad C**, **Selbekk T**, **Langø T**, **Hernes TAN**, **Olav Leira H**, **Unsgård G**, **Lindseth F.** CustusX: an open-source research platform for image-guided therapy. *Int J Comput Assist Radiol Surg* 11: 505–519, 2016. doi:10.1007/s11548-015-1292-0.

20. **Myronenko A**, **Song X.** Point set registration: coherent point drift. *IEEE Trans Pattern Anal Mach Intell* 32: 2262–2275, 2010. doi:10.1109/TPAMI.2010.46.

21. **Donovan GM**, **Elliot JG**, **Green FH**, **James AL**, **Noble PB.** Unraveling a clinical paradox: why does bronchial thermoplasty work in asthma? *Am J Respir Cell Mol Biol* 59: 355–362, 2018. doi:10.1165/rcmb.2018-0011OC.

22. **Tawhai MH**, **Pullan A**, **Hunter P.** Generation of an anatomically based three-dimensional model of the conducting airways. *Ann Biomed Eng* 28: 793–802, 2000. doi:10.1114/1.1289457.

23. **Donovan GM**, **Elliot JG**, **Green FH**, **James AL**, **Noble PB.** Reply to: comment on "Unraveling a Clinical Paradox: Why Does Bronchial Thermoplasty Work in Asthma?" *Am J Respir Cell Mol Biol* 61: 661–663, 2019. doi:10.1165/rcmb.2019-0137LE.

24. **Donovan GM**, **Langton D**, **Noble PB.** Phenotype-and patient-specific modelling in asthma: Bronchial thermoplasty and uncertainty quantification. *J Theor Biol* 501: 110337, 2020. doi:10.1016/j.jtbi.2020.110337.

25. **Adams DC**, **Hariri LP**, **Miller AJ**, **Wang Y**, **Cho JL**, **Villiger M**, **Holz JA**, **Szabari MV**, **Hamilos DL**, **Scott Harris R**, **Griffith JW**, **Bouma BE**, **Luster AD**, **Medoff BD**, **Suter MJ.** Birefringence microscopy platform for assessing airway smooth muscle structure and function in vivo. *Sci Transl Med* 8: 359ra131, 2016. doi:10.1126/scitranslmed.aag1424.

26. **Hackmann MJ**, **Elliot JG**, **Green FH**, **Cairncross A**, **Cense B**, **McLaughlin RA**, **Langton D**, **James AL**, **Noble PB**, **Donovan GM.** Requirements and limitations of imaging airway smooth muscle throughout the lung in vivo. *Respir Physiol Neurobiol* 301: 103884, 2022. doi:10.1016/j.resp.2022.103884.

27. **Li Q**, **Karnowski K**, **Noble PB**, **Cairncross A**, **James A**, **Villiger M**, **Sampson DD.** Robust reconstruction of local optic axis orientation with fiber-based polarization-sensitive optical coherence tomography. *Biomed Opt Express* 9: 5437–5455, 2018. doi:10.1364/BOE.9.005437.

28. **Harvey BC**, **Parameswaran H**, **Lutchen KR.** Can breathing-like pressure oscillations reverse or prevent narrowing of small intact airways? *J Appl Physiol (1985)* 119: 47–54, 2015. doi:10.1152/japplphysiol.01100.2014.

29. **LaPrad AS**, **Szabo TL**, **Suki B**, **Lutchen KR.** Tidal stretches do not modulate responsiveness of intact airways in vitro. *J Appl Physiol (1985)* 109: 295–304, 2010. doi:10.1152/japplphysiol.00107.2010.

30. **Hansen L**, **Heinrich MP.** GraphRegNet: deep graph regularisation networks on sparse keypoints for dense registration of 3D lung CTs. *IEEE Trans Med Imaging* 40: 2246–2257, 2021. doi:10.1109/TMI.2021.3073986.

31. **Heinrich MP**, **Jenkinson M**, **Brady M**, **Schnabel JA.** MRF-based deformable registration and ventilation estimation of lung CT. *IEEE Trans Med Imaging* 32: 1239–1248, 2013. doi:10.1109/TMI.2013.2246577.

32. **Sarrut D**, **Baudier T**, **Ayadi M**, **Tanguy R**, **Rit S.** Deformable image registration applied to lung SBRT: usefulness and limitations. *Phys Med* 44: 108–112, 2017. doi:10.1016/j.ejmp.2017.09.121.

33. **Hashmi MD**, **Khan A**, **Shafiq M.** Bronchial thermoplasty: state of the art. *Respirology* 27: 720–729, 2022. doi:10.1111/resp.14312.

34. **Wang KC**, **Donovan GM**, **James AL**, **Noble PB.** Asthma: pharmacological degradation of the airway smooth muscle layer. *Int J Biochem Cell Biol* 126: 105818, 2020. doi:10.1016/j.biocel.2020.105818.